

# Revisiting Visual Grounding

**Erik Conser**

Computer Science Department  
Portland State University  
econser@pdx.edu

**Kennedy Hahn**

Computer Science Department  
Portland State University  
kehahn@pdx.edu

**Chandler M. Watson**

Computer Science Department  
Stanford University  
chandler.watson@stanford.edu

**Melanie Mitchell**

Computer Science Department  
Portland State University  
and Santa Fe Institute  
mm@pdx.edu

## Abstract

We revisit a particular visual grounding method: the “Image Retrieval Using Scene Graphs” (IRSG) system of Johnson et al. (2015). Our experiments indicate that the system does not effectively use its learned object-relationship models. We also look closely at the IRSG dataset, as well as the widely used Visual Relationship Dataset (VRD) that is adapted from it. We find that these datasets exhibit biases that allow methods that ignore relationships to perform relatively well. We also describe several other problems with the IRSG dataset, and report on experiments using a subset of the dataset in which the biases and other problems are removed. Our studies contribute to a more general effort: that of better understanding what machine learning methods that combine language and vision actually learn and what popular datasets actually test.

## 1 Introduction

*Visual grounding* is the general task of locating the components of a structured description in an image. In the visual-grounding literature, the structured description is often a natural-language phrase that has been parsed as a *scene graph* or as a *subject-predicate-object* triple. As one example of a visual-grounding challenge, Figure 1 illustrates the “Image Retrieval using Scene Graphs” (IRSG) task (Johnson et al., 2015). Here the sentence “A standing woman wearing dark sunglasses” is converted to a scene-graph representation (right) with nodes corresponding to objects, attributes, and relationships. Given a scene graph

and an input image, the grounding task is to create bounding boxes corresponding to the specified objects, such that the located objects have the specified attributes and relationships (left). A final energy score reflects the quality of the match between the scene graph and the located boxes (lower is better), and can be used to rank images in a retrieval task. A second example of visual grounding, illustrated in Figure 2, is the “Referring Relationships” (RR) task of Krishna et al. (2018). Here, a sentence (e.g., “A horse following a person”) is represented as a subject-predicate-object triple (“horse”, “following”, “person”). Given a triple and an input image, the task is to create bounding boxes corresponding to the named subject and object, such that the located boxes fit the specified predicate. Visual grounding tasks—at the intersection of vision and language—have become a popular area of research in machine learning, with the potential of improving automated image editing, captioning, retrieval, and question-answering, among other tasks.

While deep neural networks have produced impressive progress in object detection, visual-grounding tasks remain highly challenging. On the language side, accurately transforming a natural language phrase to a structured description can be difficult. On the vision side, the challenge is to learn—in a way that can be generalized—visual features of objects and attributes as well as flexible models of spatial and other relationships, and then to apply these models to figure out which of a given object class (e.g., *woman*) is the one referred to, sometimes locating small objects and recog-

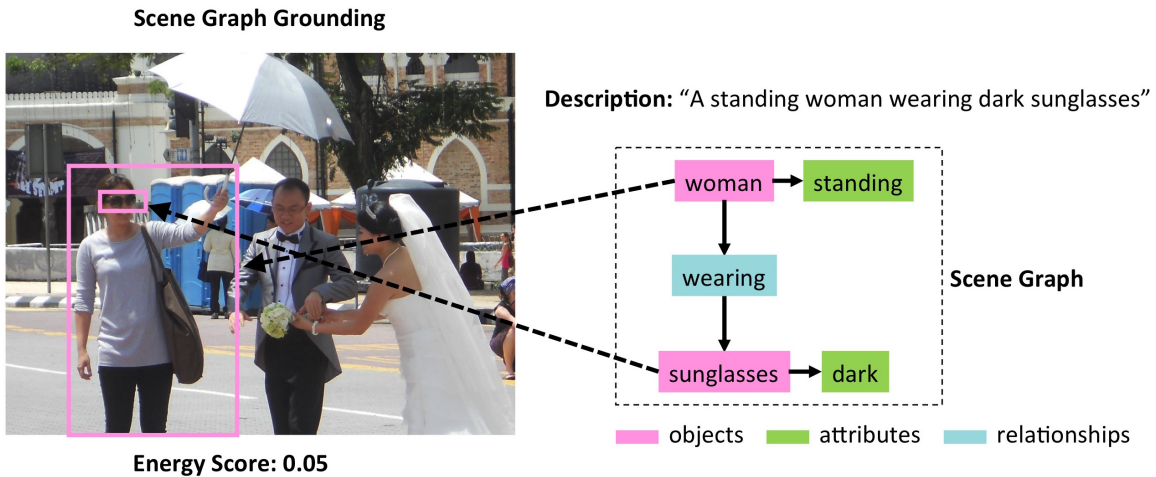


Figure 1: An example of the scene-graph-grounding task of Johnson et al. (2015). Right: A phrase represented as a scene graph. Left: A candidate grounding of the scene graph in a test image, here yielding a low energy score (lower is better).

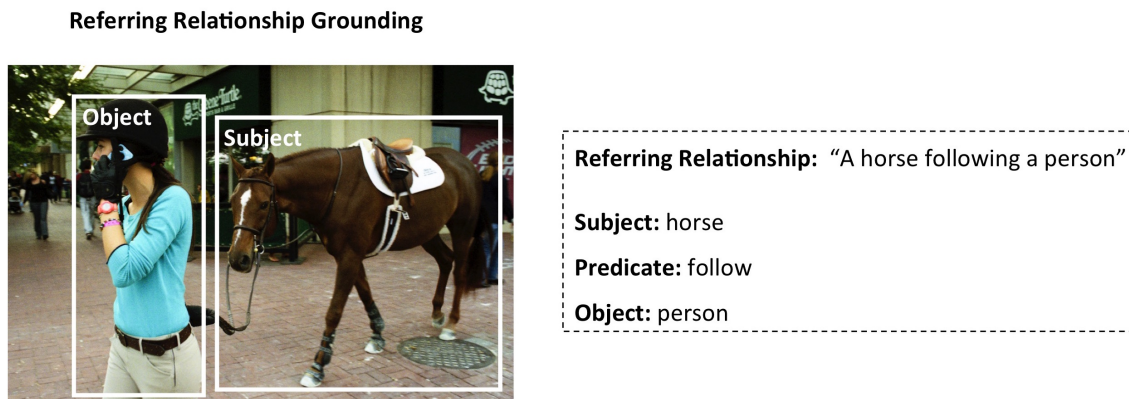


Figure 2: An example of the referring-relationship-grounding task of Krishna et al. (2018). Right: A phrase broken into subject, predicate, and object categories. Left: a candidate grounding of subject and object in a test image.

nizing hard-to-see attributes (e.g., *dark* vs. *clear* sunglasses). To date, the performance of machine learning systems on visual-grounding tasks with real-world datasets has been relatively low compared to human performance.

In addition, some in the machine-vision community have questioned the effectiveness of popular datasets that have been developed to evaluate the performance of systems on visual grounding tasks like the ones illustrated in Figures 1 and 2. Recently Cirik et al. (2018b) showed that for the widely used dataset Google-Ref (Mao et al., 2016), the task of grounding referring expressions has exploitable biases: for example, a system that predicts only object categories—ignoring relationships and attributes—still performs well on this task. Jabri et al. (2016) report related biases in visual question-answering datasets.

In this paper we re-examine the visual grounding approach of Johnson et al. (2015) to determine how well this system is actually performing scene-graph grounding. In particular, we compare this system with a simple baseline method to test if the original system is using information from object relationships, as claimed by Johnson et al. (2015). In addition, we investigate possible biases and other problems with the dataset used by Johnson et al. (2015), a version of which has also been used in many later studies. We briefly survey related work in visual grounding, and discuss possible future studies in this area.

## 2 Image Retrieval Using Scene Graphs

### 2.1 Methods

The “Image Retrieval Using Scene Graphs” (IRSG) method (Johnson et al., 2015) performs the

task illustrated in Figure 1: given an input image and a scene graph, output a *grounding* of the scene graph in the image and an accompanying energy score. The grounding consists of a set of bounding boxes, each one corresponding to an object named in the scene graph, with the goal that the grounding gives the the best possible fit to the objects, attributes, and relationships specified in the scene graph. Note that the system described in (Johnson et al., 2015) does not perform any linguistic analysis; it assumes that a natural-language description has already been transformed into a scene graph.

The IRSG system is trained on a set of human-annotated images in which bounding boxes are labeled with object categories and attributes, and pairs of bounding boxes are labeled with relationships. The system learns appearance models for all object and attribute categories in the training set, and relationship models for all training-set relationships. The appearance model for object categories is learned as a convolutional neural network (CNN), which inputs an bounding box from an image and outputs a probability distribution over all object categories. The appearance model for object attributes is also learned as a CNN; it inputs an image bounding box and outputs a probability distribution over all attribute categories. The pairwise spatial relationship models are learned as Gaussian mixture models (GMMs); each GMM inputs a pair of bounding boxes from an image and outputs a probability density reflecting how well the GMM judges the input boxes to fit the model’s corresponding spatial relationship (e.g., “woman wearing sunglasses”). Details of the training procedures are given in (Johnson et al., 2015).

After training is completed, the IRSG system can be run on test images. Given a test image and a scene graph, IRSG attempts to ground the scene graph in the image as follows. First the system creates a set of candidate bounding boxes using the Geodesic Object Proposal method (Krähenbühl and Koltun, 2014). The object and attribute CNNs are then used to assign probability distributions over all object and attribute categories to each candidate bounding box. Next, for each relationship in the scene graph, the GMM corresponding to that relationship assigns a probability density to each pair of candidate bounding boxes. The probability density is calibrated by Platt scaling (Platt, 2000) to provide a value representing the probability that the given pair of boxes is in the specified relation-

ship.

Finally, these object and relationship probabilities are used to configure a conditional random field, implemented as factor graph. The objects and attributes are unary factors in the factor graph, each with one value for each image bounding box. The relationships are binary factors, with one value for each pair of bounding boxes. This factor graph represents the probability distribution of groundings conditioned on the scene graph and bounding boxes. Belief propagation (Andres et al., 2012) is then run on the factor graph to determine which candidate bounding boxes produce the lowest-energy grounding of the given scene graph. The output of the system is this grounding, along with its energy. The lower the energy, the better the predicted fit between the image and the scene graph.

To use the IRSG system in image retrieval, with a query represented as a scene graph, the IRSG system applies the grounding procedure for the given scene graph to every image in the test set, and ranks the resulting images in order of increasing energy. The highest ranking (lowest energy) images can be returned as the results of the query.

Johnson et al. (2015) trained and tested the IRSG method on an image dataset consisting of 5,000 images, split into 4,000 training images and 1,000 testing images. The objects, attributes, and relationships in each image were annotated by Amazon Mechanical Turk workers; the authors created scene graphs that captured the annotations. IRSG was tested on two types of scene-graph queries: full and partial. Each full scene-graph query was a highly detailed description of a single image in the test set—the average full scene graph consisted of 14 objects, 19 attributes, and 22 relationships. The partial scene graphs were generated by examination of subgraphs of the full scene graphs. Each combination of two objects, one relation, and one or two attributes was drawn from each full scene graph, and any partial scene graph that was found at least five times was added to the collection of partial queries. Johnson et al. randomly selected 119 partial queries to constitute the test set for partial queries.

## 2.2 Original Results

Johnson et al. (2015) used a “recall at  $k$ ” metric to measure their their system’s image retrieval performance. In experiments on both full and partial

scene-graph queries, the authors found that their method outperformed several baselines. In particular, it outperformed—by a small degree—two “ablated” forms of their method: the first in which only object probabilities were used (attribute and relationship probabilities were ignored), and the second in which both object and attribute probabilities were used but relationship probabilities were ignored.

### 3 Revisiting IRSG

We obtained the IRSG code from the authors (Johnson et al., 2015), and attempted to replicate their reported results on the partial scene graphs. (Our study included only the partial scene graphs, which seemed to us to be a more realistic use case for image retrieval than the complex full graphs, each of which described only one image in the set.) We performed additional experiments in order to answer the following questions: (1) Does using relationship information in addition to object information actually help the system’s performance? (2) Does the dataset used in this study have exploitable biases, similar to the findings of Cirik et al. (2018b) on the Google-Ref dataset? Note that here we use the term “bias” to mean any aspect of the dataset that allows a learning algorithm to rely on shallow correlations, rather than actually solving the intended task. (3) If the dataset does contain biases, how would IRSG perform on a dataset that did not contain such biases?

#### 3.1 Comparing IRSG with an Object-Only Baseline

To investigate the first two questions, we created a baseline image-retrieval method that uses information only from object probabilities. Given a test image and a scene-graph query, we ran IRSG’s Geodesic Object Proposal method on the test image to obtain bounding boxes, and we ran IRSG’s trained CNN on each bounding box to obtain a probability for each object category. For each object category named in the query, our baseline method simply selects the bounding box with the highest probability for that query. No attribute or relationship information is used. We then use a *recall at k* ( $R@k$ ) metric to compare the performance of our baseline method to that of the IRSG method.

Our  $R@k$  metric was calculated as follows. For a given scene-graph query, let  $S_p$  be the set of *pos-*

*itive* images in the test set, where a positive image is one whose ground-truth object, attribute, and relationship labels match the query. Let  $S_n$  be the set of negative images in the test set. For each scene-graph query, IRSG was run on both  $S_p$  and  $S_n$ , returning an energy score for each image with respect to the scene graph. For each image we also computed a second score: the geometric mean of the highest object-category probabilities, as described above. The latter score ignored attribute and relationship information. We then rank-order each image in the test set by its score: for the IRSG method, scores (energy values—lower is better) are ranked in ascending order; for the baseline method, scores (geometric mean values—higher is better) are ranked in descending order. Because the size of  $S_p$  is different for different queries, we consider each positive image  $I_p \in S_p$  separately. We put  $I_p$  alone in a pool with all the negative images, and ask if  $I_p$  is ranked in the top  $k$ . We define  $R@k$  as the fraction of images in  $S_p$  that are top- $k$  in this sense. For example,  $R@1 = .2$  would mean that 20% of the positive images are ranked above all of the negative images for this query;  $R@2 = .3$  would mean that 30% of the positive images are ranked above all but at most one of the negative images, and so on. This metric is slightly different from—and, we believe, provides a more useful evaluation than—the recall at  $k$  metric used in (Johnson et al., 2015), which only counted the position of the top-ranked positive image for each query in calculating  $R@k$ .

We computed  $R@k$  in this way for each of the 150 partial scene graphs that were available in the test set provided by Johnson et al., and then averaged the 150 values at each  $k$ . The results are shown in Figure 3, for  $k = 1, \dots, 1000$ . It can be seen that the two curves are nearly identical. Our result differs in a small degree from the results reported in (Johnson et al., 2015), in which IRSG performed slightly but noticeably better than an object-only version. The difference might be due to differences in the particular subset of scene-graph queries they used (they randomly selected 119, which were not listed in their paper), or to the slightly different  $R@k$  metrics.

Our results imply that, contrary to expectations, IRSG performance does not benefit from the system’s relationship models. (IRSG performance also does not seem to benefit from the system’s attribute models, but here we focus on the role of

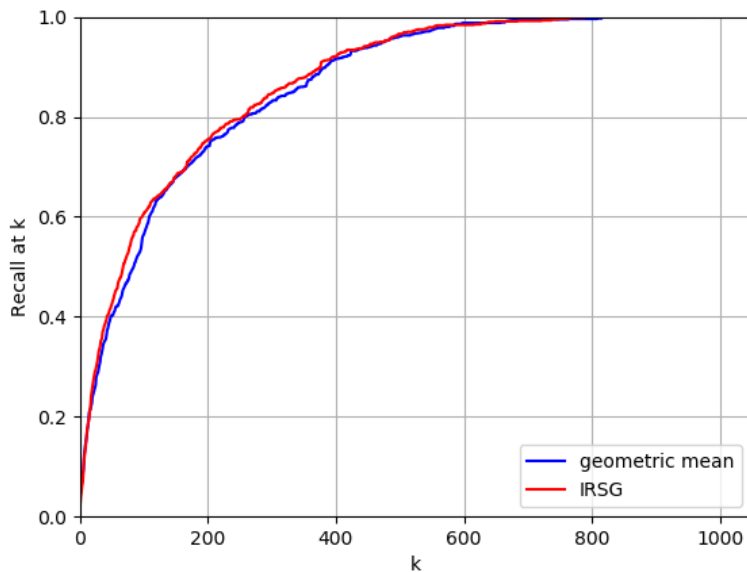


Figure 3: Recall at  $k$  values for IRSG and the geometric-mean baseline on the partial query dataset from (Johnson et al., 2015). This figure shows the averaged  $R@k$  values for all partial scene-graph queries.

relationships.) There are two possible reasons for this: (1) the object-relationship models (Gaussian mixture models) in IRSG are not capturing useful information; or (2) there are biases in the dataset that allow successful scene-graph grounding without any information from object relationships. Our studies show that both hypotheses are correct.

Figure 4 shows results that support the first hypothesis. If, for a given scene-graph query, we look at IRSG’s lowest-energy configuration of bounding boxes for every image, and compare the full (object-attribute-relationship) factorization (product of probabilities) to the factorization without relationships, we can see that the amount of information provided by the relationships is quite small. For example, for the query “clear glasses on woman”, Figure 4 is a scatter plot in which each point represents an image in the test set. The  $x$ -axis values give the products of IRSG-assigned probabilities for objects and attributes in the scene graph, and the  $y$ -axis values give the full product—that is, including the relationship probabilities. If the relationship probabilities added useful information, we would expect a non-linear relationship between the  $x$ - and  $y$ -axis values. However, the plot generally shows a simple linear relationship (linear regression goodness-of-fit  $r^2 = 0.97$ ), which indicates that the relationship distribution is not adding significant informa-

tion to the final grounding energy. We found that over 90% of the queries exhibited very strong linear relationships ( $r^2 \geq 0.8$ ) of this kind. This suggests that the relationship probabilities computed by the GMMs are not capturing useful information.

We investigated the second hypothesis—that there are biases in the dataset that allow successful object grounding without relationship information—by a manual inspection of the 150 scene-graph queries and a sample of the 1,000 test images. We found two types of such biases. In the first type, a positive test image for a given query contains only one instance of each query object, which makes relationship information superfluous. For example, when given a query such as “standing man wearing shirt” there is no need to distinguish which is the particular “standing man” who is wearing a “shirt”: there is only one of each. In the second type of bias, a positive image for a given query contains multiple instances of the query objects, but *any* of the instances would be a correct grounding for the query. For example, when given the query “black tire on road”, even if there are many different tires in the image, all of them are black and all of them are on the road. Thus any black-tire grounding will be correct. Time constraints prevented us from making a precise count of instances of these biases for each

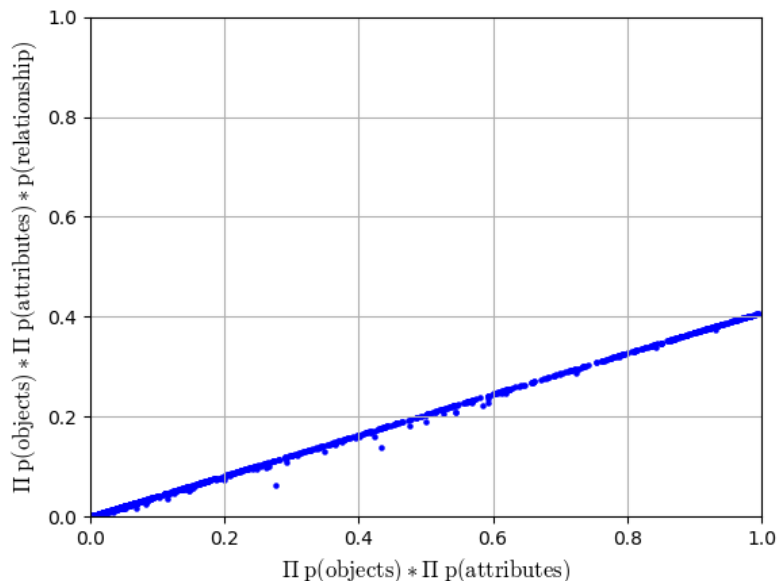


Figure 4: A scatterplot of the factorizations for a single query in the original dataset (“clear glasses on woman”), each point representing a single image. The x-axis value is the product of the object and attribute probability values from IRSG’s lowest-energy grounding on this image. The y-axis value includes the product of the relationship probabilities. A strong relationship model would modify the object-attribute factorization and create a larger spread of values than what is evident in this figure. We found similar strongly linear relationships for over 90% of the queries in the test set.

query, but our sampling suggested that examples of such biases occur in the positive test images for at least half of the queries.

A closer look at the dataset and queries revealed several additional issues that make it difficult to evaluate the performance of a visual grounding system. While Johnson et al. (2015) reported averages over many partial scene-graph queries, these averages were biased by the fact that in several cases essentially same query appeared more than once in the set, sometimes using synonymous terms (e.g., “bus on gray street” and “bus on gray road” are counted as separate queries, as are “man on bench” and “sitting man on bench”). Removing duplicates of this kind decreases the original set of 150 queries to 105 unique queries. Going further, we found that some queries included two instances of a single object class: for example, “standing man next to man”. We found that when given such queries, the IRSG system would typically create two bounding boxes around the same object in the image (e.g., the “standing man” and the other man would be grounded as the same person).

Additionally, there are typically very few positive images per query in the test set. The mean number of positive images per query is 6.5, and

the median number is 5. The dataset would benefit from a greater number of positive results for more thorough testing results.

The dataset was annotated by Amazon Mechanical Turk workers using an open annotation scheme, rather than directing the workers to select from a specific set of classes, attributes, and relationships. Due to the open scheme, there are numerous errors that affect a system’s learning potential, including mislabeled objects and relationships, as well as typographical errors (refridgerator [sic]), synonyms (kid/child, man/guy/boy/person), and many prominent objects left unlabeled. These errors can lead to false negatives during testing.

### 3.2 Testing IRSG on “Clean” Queries and Data

To assess the performance of IRSG without the complications of many of these data and query issues, we created seven queries—involving only objects and relationships, no attributes—that avoided many of the ambiguities described above. We made sure that there were at least 10 positive test-set examples for each query, and we fixed the labeling in the training and test data to make sure

that all objects named in these queries were correctly labeled. The queries (and number of positive examples for each in the test set) are the following:

- Person Has Beard: 96
- Person Wearing Helmet: 81
- Person Wearing Sunglasses: 79
- Pillow On Couch: 38
- Person On Skateboard: 29
- Person On Bench: 18
- Person On Horse: 13

We call this set of queries, along with their training and test examples, the “clean dataset”.

Using only these queries, we repeated the comparison between IRSG and the geometric-mean baseline described above. The  $R@k$  results are shown in Figure 5. These results are very similar to those in Figure 3. This result indicates that, while the original dataset exhibits biases and other problems that make the original system hard to evaluate, it still seems that relationship probabilities do not provide strongly distinguishing information to the other components of the IRSG method. The lack of strong relationship performance was also seen in (Quinn et al., 2018) where the IRSG and object-only baseline method showed almost identical  $R@k$  performance on a different, larger dataset.

#### 4 Revisiting “Referring Relationship” Grounding

The IRSG task is closely related to the “Referring Relationships” (RR) task, proposed by Krishna et al. (2018) and illustrated in Figure 2. The method developed by Krishna et al. uses iterative attention to shift between image regions according to the given predicate, in order to locate subject and object. The authors evaluated their model on several datasets, including the same images as were in the IRSG dataset (here called “VRD” or “visual relationship dataset”), but with 4710 referring-relationship queries (several per test image). The evaluation metric they reported was mean *intersection over union* (IOU) of the subject and object detections with ground-truth boxes. This metric does not give information about the

detection rate. To investigate whether biases appear in this dataset and queries similar to the ones we described above, we again created a baseline method that used only object information. In particular, we used the VRD training set to fine-tune a pre-trained version<sup>1</sup> of the faster-RCNN object-detection method (Ren et al., 2015) on the object categories that appear in the VRD dataset. We then ran faster-RCNN on each test image, and for each query selected the highest-confidence bounding box for the subject and object categories. (If the query subject and object were the same category, we randomly assigned subject and object to the highest and second-highest confidence boxes.) Finally, for each query, we manually examined visualizations of the predicted subject and object boxes in each test image to determine whether the subject and object boxes fit the subject, object, and predicate of the query. We found that for 56% of the image/query pairs, faster-RCNN had identified correct subject and object boxes. In short, our object-only baseline was able to correctly locate the subject and object 56% of the time, using no relationship information. This indicates significant biases in the dataset, which calls into question any published referring-relationship results on this dataset that does not compare with this baseline. In future work we plan to replicate the results reported by Krishna et al. (2018) and to compare it with our object-only baseline. We hope to do the same for other published results on referring relationships using the VRD dataset, among other datasets (Cirik et al., 2018a; Liu et al., 2019; Raboh et al., 2019).

#### 5 Related Work

Other groups have explored grounding single objects referred to by natural-language expressions (Hu et al., 2016; Nagaraja et al., 2016; Hu et al., 2017; Zhang et al., 2018) and grounding all nouns mentioned in a natural language phrase (Rohrbach et al., 2016; Plummer et al., 2017, 2018; Yeh et al., 2017).

Visual grounding is different from, though related to, tasks such as visual relationship detection (Lu et al., 2016), in which the task is not to ground a particular phrase in an image, but to detect *all* known relationships. The VRD dataset we

<sup>1</sup>We used `faster_rcnn_resnet101_coco` from [https://github.com/tensorflow/models/blob/master/research/object\\_detection/g3doc/detection\\_model\\_zoo.md](https://github.com/tensorflow/models/blob/master/research/object_detection/g3doc/detection_model_zoo.md).

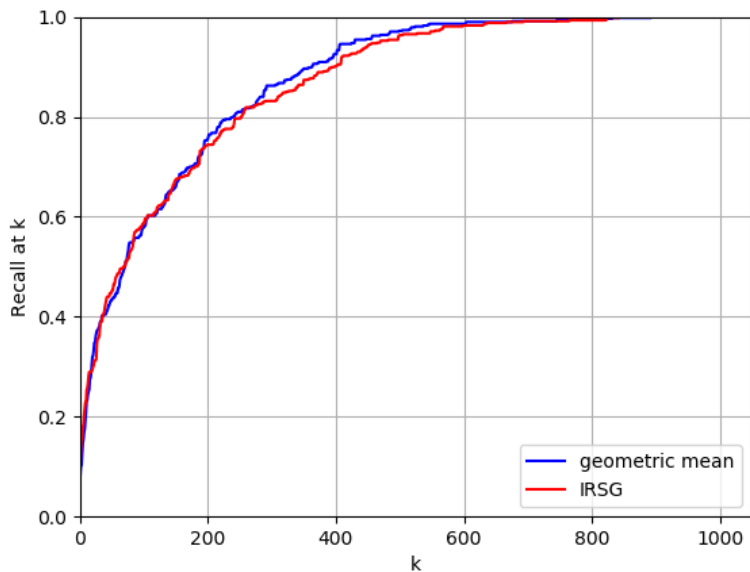


Figure 5:  $R@k$  values for the IRSG model and geometric mean model on the clean dataset. This figure shows, for each  $k$ , the averaged  $R@k$  values over the seven queries.

described above is commonly used in visual relationship detection tasks, and to our knowledge there are no prior studies of bias and other problems in this dataset.

It should be noted that visual grounding also differs from automated caption generation (Xu et al., 2015) and automated scene graph generation (Xu et al., 2017), which input an image and output a natural language phrase or a scene graph, respectively.

The diversity of datasets used in these various studies as well as the known biases and other problems in many widely used datasets makes it difficult to determine the state of the art in visual grounding tasks as well as related tasks such as visual relationship detection.

## 6 Conclusions and Future Work

We have closely investigated one highly cited approach to visual grounding, the IRSG method of (Johnson et al., 2015). We demonstrated that this method does not perform better than a simple object-only baseline, and does not seem to use information from relationships between objects, contrary to the authors’ claims, at least on the original dataset of partial scene graphs as well as on our “clean” version. We have also identified exploitable biases and other problems associated with this dataset, as well as with the version used

in Krishna et al. (2018).

Our work can be seen as a contribution to the effort promoted by Cirik et al. (2018b): “to make meaningful progress on grounded language tasks, we need to pay careful attention to what and how our models are learning, and whether or datasets contain exploitable bias.” In future work, we plan to investigate other prominent algorithms and datasets for visual grounding, as well as to curate benchmarks without the biases and problems we described above. Some researchers have used synthetically generated data, such as the CLEVR set (Johnson et al., 2017); however to date the high performances of visual grounding systems on this dataset have not translated to high performance on real-world datasets (e.g., Krishna et al. (2018)). We also plan to explore alternative approaches to visual grounding tasks, such as the “active” approach described by Quinn et al. (2018).

## Acknowledgments

We are grateful to Justin Johnson of Stanford University for sharing the source code for the IRSG project, and to NVIDIA corporation for donation of a GPU used for this work. We also thank the anonymous reviewers of this paper for several helpful suggestions for improvement. This material is based upon work supported by the National Science Foundation under Grant Number



IIS-1423651. Any opinions, findings, and conclusions or recommendations expressed in this material are those of the authors and do not necessarily reflect the views of the National Science Foundation.

## References

- Bjoern Andres, Thorsten Beier, and Jörg H. Kappes. 2012. OpenGM: A C++ library for discrete graphical models. *arXiv preprint arXiv:1206.0111*.
- Volkan Cirik, Taylor Berg-Kirkpatrick, and Louis-Philippe Morency. 2018a. Using syntax to ground referring expressions in natural images. In *Proceedings of the Thirty-Second Conference on Artificial Intelligence (AAAI)*, pages 6756–6764. AAAI.
- Volkan Cirik, Louis-Philippe Morency, and Taylor Berg-Kirkpatrick. 2018b. Visual referring expression recognition: What do systems actually learn? In *Proceedings of NAACL-HLT 2018*, pages 781–787.
- Ronghang Hu, Marcus Rohrbach, Jacob Andreas, Trevor Darrell, and Kate Saenko. 2017. Modeling relationships in referential expressions with compositional modular networks. In *Proceedings of the IEEE Conference on Computer Vision and Pattern Recognition (CVPR)*, pages 1115–1124.
- Ronghang Hu, Huazhe Xu, Marcus Rohrbach, Jiashi Feng, Kate Saenko, and Trevor Darrell. 2016. Natural language object retrieval. In *Proceedings of the IEEE Conference on Computer Vision and Pattern Recognition*, pages 4555–4564.
- Allan Jabri, Armand Joulin, and Laurens Van Der Maaten. 2016. Revisiting visual question answering baselines. In *European Conference on Computer Vision (ECCV)*, pages 727–739. Springer.
- Justin Johnson, Bharath Hariharan, Laurens van der Maaten, Li Fei-Fei, C Lawrence Zitnick, and Ross Girshick. 2017. CLEVR: A diagnostic dataset for compositional language and elementary visual reasoning. In *Proceedings of the IEEE Conference on Computer Vision and Pattern Recognition (CVPR)*, pages 2901–2910.
- Justin Johnson, Ranjay Krishna, Michael Stark, Li-Jia Li, David Shamma, Michael Bernstein, and Li Fei-Fei. 2015. Image retrieval using scene graphs. In *Proceedings of the IEEE Conference on Computer Vision and Pattern Recognition (CVPR)*, pages 3668–3678.
- Philipp Krähenbühl and Vladlen Koltun. 2014. Geodesic object proposals. In *Proceedings of the European Conference on Computer Vision (ECCV)*, pages 725–739.
- Ranjay Krishna, Ines Chami, Michael Bernstein, and Li Fei-Fei. 2018. Referring relationships. In *Proceedings of the IEEE Conference on Computer Vision and Pattern Recognition (CVPR)*, pages 6867–6876.
- Xihui Liu, Wang Zihao, Jing Shao, Xiaogang Wang, and Hongsheng Li. 2019. Improving referring expression grounding with cross-modal attention-guided erasing. *arXiv preprint arXiv:1903.00839*.
- Cewu Lu, Ranjay Krishna, Michael Bernstein, and Li Fei-Fei. 2016. Visual relationship detection with language priors. In *European Conference on Computer Vision (ECCV)*, pages 852–869. Springer.
- Junhua Mao, Jonathan Huang, Alexander Toshev, Oana Camburu, Alan L. Yuille, and Kevin Murphy. 2016. Generation and comprehension of unambiguous object descriptions. In *Proceedings of the IEEE Conference on Computer Vision and Pattern Recognition (CVPR)*, pages 11–20.
- Varun K. Nagaraja, Vlad I. Morariu, and Larry S. Davis. 2016. Modeling context between objects for referring expression understanding. In *European Conference on Computer Vision (ECCV)*, pages 792–807. Springer.
- John C. Platt. 2000. Probabilistic outputs for support vector machines and comparisons to regularized likelihood methods. In *Advances in Large Margin Classifiers*. MIT Press.
- Bryan A. Plummer, Arun Mallya, Christopher M. Cervantes, Julia Hockenmaier, and Svetlana Lazebnik. 2017. Phrase localization and visual relationship detection with comprehensive image-language cues. In *Proceedings of the IEEE International Conference on Computer Vision*, pages 1928–1937.
- Bryan A. Plummer, Kevin J. Shih, Yichen Li, Ke Xu, Svetlana Lazebnik, Stan Sclaroff, and Kate Saenko. 2018. Open-vocabulary phrase detection. *arXiv preprint arXiv:1811.07212*.
- Max H. Quinn, Erik Conser, Jordan M. Witte, and Melanie Mitchell. 2018. Semantic image retrieval via active grounding of visual situations. In *International Conference on Semantic Computing (ICSC)*, pages 172–179. IEEE.
- Moshiko Raboh, Roei Herzig, Gal Chechik, Jonathan Berant, and Amir Globerson. 2019. Learning latent scene-graph representations for referring relationships. *arXiv preprint arXiv:1902.10200*.
- Shaoqing Ren, Kaiming He, Ross Girshick, and Jian Sun. 2015. Faster R-CNN: Towards real-time object detection with region proposal networks. In *Advances in Neural Information Processing Systems*, pages 91–99.
- Anna Rohrbach, Marcus Rohrbach, Ronghang Hu, Trevor Darrell, and Bernt Schiele. 2016. Grounding of textual phrases in images by reconstruction. In

*European Conference on Computer Vision (ECCV)*, pages 817–834. Springer.

Danfei Xu, Yuke Zhu, Christopher B. Choy, and Li Fei-Fei. 2017. Scene graph generation by iterative message passing. In *Proceedings of the IEEE Conference on Computer Vision and Pattern Recognition*, pages 5410–5419.

Kelvin Xu, Jimmy Ba, Ryan Kiros, Kyunghyun Cho, Aaron Courville, Ruslan Salakhudinov, Rich Zemel, and Yoshua Bengio. 2015. Show, attend and tell: Neural image caption generation with visual attention. In *International conference on machine learning*, pages 2048–2057.

Raymond Yeh, Jinjun Xiong, Wen-Mei Hwu, Minh Do, and Alexander Schwing. 2017. Interpretable and globally optimal prediction for textual grounding using image concepts. In *Advances in Neural Information Processing Systems*, pages 1912–1922.

Hanwang Zhang, Yulei Niu, and Shih-Fu Chang. 2018. Grounding referring expressions in images by variational context. In *Proceedings of the IEEE Conference on Computer Vision and Pattern Recognition*, pages 4158–4166.